CLM-P776

NUMERICAL SIMULATION OF ONE-DIMENSIONAL MULTIPHASE MIXING

D.F.Fletcher and A.Thyagaraja
UKAEA, Culham Laboratory,
Abingdon, Oxon, OX14 3DB, U.K.

ABSTRACT

In this paper we extend an algorithm used for calculating two-phase fluid flow to model the situation which occurs when a hot liquid is poured into a cooler volatile liquid leading to vapour generation. This has required the development of a transient, 3 phase Eulerian finite difference code. The code has been compared with results from one-dimensional mixing experiments and has been used to examine the effect of varying the ambient pressure.

(To be submitted to International Journal for Numerical Methods in Engineering)

August, 1986

1. Introduction

In this paper we report on the development of a one-dimensional, multiphase code described in our previous work [1]. The purpose of this code is to study the transient, buoyancy-driven mixing processes which occur on relatively slow timescales (~ 1 second) when a hot liquid (e.g. molten aluminium) is poured into a pool of cold vaporisable liquid (e.g. water). This situation occurs in certain industrial processes [2], volcanisms [3], and could arise during the progression of accidents in nuclear reactors if core material melts and pours into liquid coolant [4].

At present the detailed physics of this process is relatively poorly understood [5]; for example the details of the heat transfer and momentum exchange processes are not known and there is no established theory which enables length-scales of the various components to be determined with any precision. Thus, we are concerned only with modelling some of the features of mixing, using a one-dimensional, multi-phase, continuum description. Whereas our earlier paper dealt with two-phase hydrodynamics, the present work extends the methods to three components, including the possibility of phase transformations.

The paper is organised as follows: in Section 2 the analytic formulation of the problem is given. This includes the complete set of equations solved, together with the initial and boundary conditions needed to completely specify the problem. A brief discussion of the physical approximations implicit in the model is also given. Section 3 is devoted to an exposition of the numerical treatment of the problem. While we draw heavily on our earlier paper, the specific new features needed in the present extension are highlighted and discussed in detail. Section 4 contains the presentation of results obtained with the present code on test cases. These test examples include comparison with experimental data. Section 5 presents a discussion and conclusions.

2. Analytic Formulation

Following our earlier work [1], we consider the one-dimensional,

transient, mixing problem in a cylindrical vessel of radius R and height H . To avoid cumbersome notation, we specifically consider the mixing of two components, "melt" (usually a molten metal or metal-oxide in liquid form at a high temperature ~ 3000 K) and "coolant" (usually water). The coolant is assumed to exist in both its liquid and vapour phases. In order to simplify the problem, we assume that the melt temperature is not substantially decreased during the mixing as heat is transferred to the water which in turn is converted to steam. We further assume the coolant to be saturated and therefore neglect the condensation of steam, which is allowed to escape from the top of the vessel. The flow is essentially driven by the buoyancy forces and the steam production. Taking y as the independent variable along the vertical direction, the following dependent variables are needed in the complete fluid dynamic description of the system:

The volume fractions: $\alpha_M(y,t)$, $\alpha_W(y,t)$ and $\alpha_S(y,t)$.

The velocities: $V_M(y,t)$, $V_W(y,t)$ and $V_S(y,t)$.

The hydrostatic, common pressure $p(y,t)$.

As in our earlier work, it is reasonable to restrict ourselves to the incompressible equations of motion, taking the densities ρ_M, ρ_W and ρ_S as specified constants. It is also convenient to introduce the reduced pressure $\bar{p}(y,t)$ defined by the equation,

$$\bar{p}(y,t) = p(y,t) - \int_y^H g(\rho_M \alpha_M + \rho_W \alpha_W + \rho_S \alpha_S)dy \qquad (2.1)$$

where g is the acceleration due to gravity. The seven dependent variables defined above satisfy the following seven governing equations.

$$\alpha_M + \alpha_W + \alpha_S = 1 \qquad (2.2)$$

$$\frac{\partial \alpha_M}{\partial t} + \frac{\partial}{\partial y}(\alpha_M V_M) = 0 \qquad (2.3)$$

$$\frac{\partial \alpha_W}{\partial t} + \frac{\partial}{\partial y}(\alpha_W V_W) = \frac{\dot{m}_W}{\rho_W} \tag{2.4}$$

$$\frac{\partial \alpha_S}{\partial t} + \frac{\partial}{\partial y}(\alpha_S V_S) = \frac{\dot{m}_s}{\rho_S} \tag{2.5}$$

$$\begin{aligned}\frac{\partial}{\partial t}(\rho_M \alpha_M V_M) + \frac{\partial}{\partial y}(\rho_M \alpha_M V_M^2) = &- \alpha_M \frac{\partial \bar{p}}{\partial y} + g\alpha_M \alpha_W(\rho_W - \rho_M) \\ &+ g\alpha_M \alpha_S(\rho_S - \rho_M) \\ &+ F_{MW} + F_{MS}\end{aligned} \tag{2.6}$$

$$\begin{aligned}\frac{\partial}{\partial t}(\rho_W \alpha_W V_W) + \frac{\partial}{\partial y}(\rho_W \alpha_W V_W^2) = &-\alpha_W \frac{\partial \bar{p}}{\partial y} + g\alpha_W \alpha_M(\rho_M - \rho_W) \\ &+ g\alpha_W \alpha_S(\rho_S - \rho_W) \\ &+ F_{WS} + F_{WM} + F_{W\dot{m}}\end{aligned} \tag{2.7}$$

$$\begin{aligned}\frac{\partial}{\partial t}(\rho_S \alpha_S V_S) + \frac{\partial}{\partial y}(\rho_S \alpha_S V_S^2) = &-\alpha_S \frac{\partial \bar{p}}{\partial y} + g\alpha_S \alpha_M(\rho_M - \rho_S) \\ &+ g\alpha_S \alpha_W(\rho_W - \rho_S) \\ &+ F_{SM} + F_{SW} + F_{S\dot{m}}\end{aligned} \tag{2.8}$$

Several comments are in order with regard to the above system.

(i) We have assumed that there are no volume sources or sinks of melt within the solution domain. Thus, in our model, the distribution in y of α_M, V_M will be specified at t = 0, subject to $V_M(0,t) = 0$ (impermeable bottom) and $\frac{\partial V_M(H,t)}{\partial y} = 0$ with the proviso that $\alpha_M(y,t) = 0$ for $y > H$. This means we allow for the possibility of a melt flux <u>out</u> of the system but do not permit any inflow. Thus in the problems we consider in this

paper no melt is introduced from any boundary into the system for the whole duration of the calculation.

(ii) We assume that $\dot{m}_W + \dot{m}_S = 0$ and also that

$$\dot{m}_W \equiv -\alpha_W(y,t)\,\alpha_M(y,t)\,\rho_S\,\lambda \tag{2.9}$$

where the positive rate function λ is a prescribed function depending on the heat transfer mechanisms. The precise prescription used in our calculations is described in the Appendix.

(iii) The boundary conditions for water are similar to those for the melt. $V_W(0,t) = 0$ and $\dfrac{\partial V_W(H,t)}{\partial y} = 0$ ($\alpha_W = 0$ for $y > H$). At $t = 0$, the water is assumed to be at rest and in equilibrium in a pool filling the lower part of the vessel into which the melt is poured. As for the melt we assume that no water is introduced into the system for the whole duration of the calculation.

(iv) Equations (2.2) to (2.5) entail the global 'continuity' relation,

$$(\alpha_M V_M + \alpha_W V_W + \alpha_S V_S)_{y=H} = \int_o^H \alpha_W \alpha_M \lambda \left(1 - \frac{\rho_S}{\rho_W}\right) dy \tag{2.10}$$

This relation, together with the other conditions, essentially determines the steam velocity (and flux) out of the system.

(v) The drag forces satisfy Newton's third law:

$$F_{MW} + F_{WM} = 0$$

$$F_{MS} + F_{SM} = 0$$

$$F_{SW} + F_{WS} = 0.$$

In general, $F_{ij} \equiv \rho_i \rho_j \alpha_i \alpha_j \left|V_i - V_j\right| (V_j - V_i) h_{ij}$ where h_{ij} depends on

$\rho_i, \rho_j, \alpha_i, \alpha_j$, and certain length scales. The Appendix gives the formulae used in the present simulation.

(vi) The forces $F_{W\dot{m}}$, $F_{S\dot{m}}$ are treated exactly as in our earlier paper $F_{W\dot{m}} + F_{S\dot{m}} = 0$, $F_{S\dot{m}} = \dot{m}_S V_W$.

(vii) The 'resultant' buoyancy forces such as $g\alpha_W\alpha_M(\rho_M - \rho_W)$ clearly cancel in pairs when equations (2.6), (2.7), and (2.8) are added.

(viii) Turbulent drag terms are not explicitly present. They are partially included in the inter-component drag terms F_{ij}.

This completes the formulation of the initial-boundary value problem. It should be noted that the boundary conditions at y = H are different to those employed in our earlier report which would have suggested $V_W = V_M = V_S$ at y = H. It should also be noted that for those problems (somewhat artificial, it must be admitted) in which $\dot{m}_S \equiv 0$, the boundary conditions change. In these cases, Eq.(2.10) clearly suggests $V_W = V_M = V_S = 0$ at y = H, as the appropriate condition.

3. Numerical Solution

The numerical solution of equations (2.1) - (2.8) closely follows the scheme introduced in our earlier paper [1]. Thus, the solution of the momentum equations (2.6) - (2.8) and the 'pressure-correction' equation,

$$\frac{\partial}{\partial y}\left\{\alpha_M V_M + \alpha_W V_W + \alpha_S V_S\right\} = \frac{\dot{m}_W}{\rho_W} + \frac{\dot{m}_S}{\rho_S} \qquad (3.1)$$

for obtaining V_M, V_W, V_S and $\bar{p}$ at t + Δt given their values at t as well as the α's at t+Δt, is exactly the same as the iterative technique described in our previous paper. The new features occur in the solution of equations (2.2) to (2.5) and in the treatment of the boundary conditions at y = H.

As discussed in Section 2, we employ the following 'outlet' boundary

conditions at y = H, assuming $\dot{m}_S$ not identically zero, $V_W(y=H) = V_W(y = H-\Delta y)$, $V_M(y=H) = V_M(y=H-\Delta y)$, where Δy is the mesh size. Furthermore, $\alpha_W(y=H+\frac{\Delta y}{2}) = \alpha_M(y=H+\frac{\Delta y}{2}) \equiv 0$. This ensures that there is no flux of water or melt <u>into</u> the solution domain. It must be remembered that we use a 'staggered-grid' such that $\alpha_W(y=H+\frac{\Delta y}{2})$ would be used to form the flux if $V_W(y=H)<0$. These conditions imply: (1) the melt has no internal sources or sinks and can only <u>leave</u> the system, (if $V_M(y=H)>0$); $Q_M = \frac{1}{H}\int_o^H \alpha_M(y,t)dy$ (Global melt occupancy) can only decrease with time, (2) the water can be transformed into steam and can only <u>leave</u> the system (if $V_W(y=H)>0$); $Q_W = \frac{1}{H}\int_o^H \alpha_W(y,t)dy$ (Global water occupancy) can only decrease with time. The boundary conditions for α_S and V_S are obtained as follows integrating equation (3.1),

$$\{\alpha_S V_S + \alpha_M V_M + \alpha_W V_W\}_{y=H} = \int_o^H \alpha_W \alpha_M \lambda(1 - \frac{\rho_S}{\rho_W})dy. \qquad (3.2)$$

Setting $\alpha_S(y=H+\frac{\Delta y}{2}) = 1$ (this is the only value consistent with (2.2) and the conditions on α_M, α_W), and knowing the value $\alpha_S(y = H - \frac{\Delta y}{2})$, (this is an 'interior' point), we get $V_S(y=H)$. We note that since V_S is non-negative in our simulation $\alpha_S(y = H + \frac{\Delta y}{2})$ is never actually needed in the calculation.

Turning to the solution of equations (2.3) - (2.5) we adopt the following procedure which ensures that $\alpha_M, \alpha_W, \alpha_S$ satisfy (2.2) and are non-negative quantities at all times. Since the melt has no sources and sinks and the melt velocities are the smallest of the three components, equation (2.3) is used to time advance α_M. Thus, using the known values of $\alpha_M(y,t)$ and $V_M(y,t)$, the explicit time-marching procedure (using the concept of positive-faithful transformations) described in our previous paper gives $\alpha_M(y,t+\Delta t)$. The boundary conditions and the solution method automatically ensure that all the α_M's so calculated are non-negative, less than unity and furthermore, $Q_M(t+\Delta t) = \frac{1}{H}\int_o^H \alpha_M(y,t+\Delta t)dy \leq Q_M(t) =$

$\frac{1}{H}\int_o^H \alpha_M(y,t)dy$. Having obtained α_M, we proceed to equation (2.4). In this equation, the advection terms are treated explicitly and exactly as in (2.3). The term on the right hand side is a sink term, which is handled implicitly, as follows. Thus, at $y = j\Delta y$,

$$\alpha_W(j,n+1)-\alpha_W(j,n) + \frac{\Delta t}{\Delta y}\{(\alpha_W V_W)^+ - (\alpha_W V_W)^-\}_n$$

$$= - \alpha_W(j,n+1)\alpha_M(j,n+1)\lambda_j \Delta t \ (1- \frac{\rho_S}{\rho_W}) \qquad (3.3)$$

where $\alpha_W(j,n+1)$ denotes $\alpha_W(j\Delta y, t+\Delta t)$.
Solving for $\alpha_W(j,n+1)$ we get

$$\alpha_W(j,n+1) = \frac{\left[\alpha_W(j,n) - \frac{\Delta t}{\Delta y}\{(\alpha_W V_W)^+ - (\alpha_W V_W)^-\}_n\right]}{\left(1 + \alpha_M(j,n+1)\lambda_j \Delta t(1 - \frac{\rho_S}{\rho_W})\right)} \qquad (3.4)$$

Since we have already calculated $\alpha_M(j,n+1)$ by solving (2.3), the denominator in (3.4) is well-defined and is always larger than unity. For accuracy, $\lambda_j \Delta t << 1$ is required. Equation (3.4) says that $\alpha_W(j,n+1)$ is smaller than the value it would have had in the absence of the sink term. We have now calculated α_M and α_W at $t+\Delta t$. α_S at $t+\Delta t$ follows from equation (2.2). From the way in which the solution is arranged, it is clear that in the absence of all velocities, the scheme only leads to non-negative volume fractions satisfying (2.2). The 'pressure-correction' equation ensures that the solutions remain consistent even when considerable velocities are generated. With minor modifications, the code can be run with the source terms set to zero. Indeed, it has been run this way to check the invariance of Q_M, Q_S and Q_W and the sum $Q_M + Q_S + Q_W$, when there are no sources.

4. Comparison with Experiments

In this section we compare the code predictions with results of experiments carried out to study mixing and use the code to make predictions about the effect of ambient pressure on mixing.

4.1 BNL Steam-spike Experiments

A one-dimensional experiment has been carried out at Brookhaven National Laboratory (BNL) [6] to study the transient behaviour of heated solid particles dropped into water. The experiments involved dropping 10kg of 3mm diameter stainless steel shot at 973K into saturated water at 373K. The mixing vessel was cylindrical (diameter 152mm, height 3m) and a water depth of 500mm was used. The velocity of the hot particles was measured to be 4.9m/s just prior to entry in the water.

The leading edge of the particle front reached the base of the vessel at about 0.2s after contact with the water. Motion pictures of the experiments showed that only one-third of the particles entered the water and generated steam. The remaining two-thirds were swept upwards by the escaping steam at about 0.6s after the particles contacted the water.

These experiments are particularly suitable for code validation since they are essentially 1D, there is no fragmentation of the 'melt' so that the heat transfer surface area per unit volume of melt is known, and the steam production rate was measured. The following modelling assumptions were made:

(i) A particle volume (packing) fraction was picked and the initial velocity of the particles was chosen so that the correct entry velocity was achieved.

(ii) The melt length-scale D_M was set equal to 3mm and D_W and D_S were set equal to the vessel diameter. All the drag coefficients were set equal and varied over the range 0.2 - 1.0 (see Appendix 1).

(iii) Heat transfer was assumed to be through blackbody radiation and convective film boiling (this was modelled using the correlation proposed by Witte [7]). Note that due to the form of the assumed vapour production source term, the heat fluxes were weighted by a factor α_W to account for the reduction in heat transfer as the water fraction falls. This set of assumptions implies that

$$\lambda = 6\left\{\sigma\left(T_M^4 - T_W^4\right) + 2.98\left[\frac{\rho_S k_S \left(h_{fg} + 0.68 C_{p_S}\left(T_M - T_W\right)\right)\left|U_M - U_W\right|}{D_M\left(T_M - T_W\right)}\right]^{1/2} \cdot \left(T_M - T_W\right)\right\} / D_M h_{fg} \rho_S \qquad (4.1)$$

and $\dot{m}_S = \alpha_W \alpha_M \rho_S \lambda$. See Appendix for further details.

(iv) The particle temperature was calculated by carrying out a lumped energy balance on the system.

(v) The computational domain was 3m in length with a continuity cell size of 0.1m and a time-step of 5×10^{-5} s was used.

Simulations were performed using the present model for initial particle volume fractions of 0.0457, 0.0572 and 0.0686, corresponding to interparticle distances of 8.3mm, 7.6mm and 7.2mm, respectively. For these calculations the drag coeeficients were set equal to 0.2, as this value was found to give good agreement with the experimentally measured time for the particles to reach the vessel base. Typically the melt volume fraction in the bottom cell was 2% after 0.2 seconds. A comparison of the transient steam flow rate predictions with the measured experimental data is shown in Figure 4.1(a). The calculations show good agreement with the experimental data for the first second of the transient. The results show that increasing the initial melt volume fraction leads to higher steam production rates because melt enters the water more quickly but this high production rate in turn leads to rapid dispersal of the mixture followed by a fall in the steam production rate. At later times the predicted steam flow rate is too low because in the

computations the melt settles too quickly relative to experiment leading to poor mixing.

The rate at which settling occurs is apparently very dependent on the magnitude of the drag coefficients. Figure 4.1(b) shows the effect of varying the drag coefficient over the range 0.2 to 1.0, for an initial melt volume fraction of 0.0572. Increasing the drag coefficients initially slows down the fall of the melt into the water but increases the time over which steam is produced rapidly. This is because the water and melt are dragged upwards more strongly. To model the later stages of the experiment more accurately, improved drag laws are needed; for example, it is well-known that drag coefficients depend on the particle volume fraction in fluidized beds [2]. Furthermore, the water length-scale also needs to be varied with time. In addition, the present model treats the melt as a fluid so that the upper bound on the melt volume fraction in a cell is unity rather than a lower value (~ 0.6) appropriate for solid particles.

The initial part of the transient (the first 0.2s) is most closely reproduced by assuming an initial particle fraction of 0.0686. Chu and Corradini [8] have also attempted to model these experiments using their mixing code and found that the initial behaviour was best reproduced using a particle volume fraction of 0.091, which is similar to the value used in the present simulation. Unfortunately, they only published their results for times upto 0.14s so it is not possible to make detailed comparisons of their results with ours.

To summarise this section we note:-

(i) The model accounts for a particle fall time close to that observed experimentally for physically reasonable choices for the initial melt fraction ($0.0457 \leq \alpha_m \leq 0.0686$) and the drag coefficients ($0.2 \leq C_D \leq 1.0$).

(ii) The predicted steam flow rates are in good general agreement with the experiments, especially during the initial mixing stage. Although the agreement between the present theory and experiment for longer times (> 1

second) is less satisfactory, the differences are clearly related to features not taken into account in the present model. These could be any one of, or all of, the following: continuum model versus finite sized particles; inadequate knowledge of drag laws as functions of volume fraction; order of magnitude knowledge only of heat transfer and steam production rate.

(iii) We note that the "free parameters" α_m (at t=0) and C_D are determined with reference to experiment by the particle fall time and the height of the initial peak in Figure 4.1(a). The shape of the steam flow rate curve is a prediction of the code which is in good qualitative agreement with experiment. Even for long times, the discrepancy is less than a factor of two and is therefore consistent with the lack of knowledge inherent in the constitutive relations.

(iv) In the calculations, levitation of the particles and liquid is very important. The degree of levitation depends strongly on the choice of initial melt volume fractions and drag coefficients.

(v) The calculations show that the steam and water velocities are, in general, very different with typical steam velocities of 10-20 m/s compared to water velocities of 0.5 - 3m/s. This suggests that the homogeneous treatment of the coolant phases, where the water and steam have the same velocity, as advocated by Bankoff and co-workers [9,10], could be a grossly misleading approximation.

4.2 The Effect of Ambient Pressure on Mixing

In this section we examine the effect of ambient pressure on mixing. Experiments have established [11] that this parameter is particularly important in determining the form and extent of the region of mixture which develops when a hot melt and vaporisable liquid come into contact. In this section we make some scoping calculations for the situation of a one dimensional pour of molten material into a cylindrical vessel partially filled with water. The following assumptions are made:

(i) A melt particle size of 10mm is used and there is no further fragmentation. The length-scales of the water and steam are set arbitrarily to 0.1m and all the drag coefficients are set to 0.5.

(ii) The melt temperature remains constant at 3000K and the heat flux is due solely to graybody radiation (emissivity = 0.84). The coolant is saturated and all the heat transferred from the melt produces saturated steam.

(iii) The vessel is 2m in diameter and 3m high. The water pool is initially 1.5m deep and 11 tonnes of molten UO_2 is poured in with an initial melt volume fraction of 0.4, and an initial velocity of 5m/s. A time-step of 5×10^{-5}s is used and the finite difference grid is composed of 30 continuity cells.

Calculations were carried out for ambient pressures in the range 0.1MPa to 15MPa. Some of the main features of the results are shown in Table 4.1. The data in the table shows that changing the pressures has a significant effect on the steam production rate and the hydrodynamics of the system. The data describing the steam production after one second of mixing is displayed in Figure 4.2, which shows that whereas the total mass of steam produced increases with pressure, there is a dramatic fall in the volume of steam produced. There is a reduction in steam volume produced by a factor of 3 for a change in pressure from 0.1MPa to 1.0MPa because of the large change in the density of steam (from 0.6kg/m^3 to 5kg/m^3). This effect has been observed experimentally over this pressure range [11].

The data shown in Table 4.1 shows that the effect of pressure on the volume of steam produced affects the velocities of the various components. The steam velocity at exit falls from 50m/s at 0.1MPa to only 3m/s at 15MPa. Thus increasing the pressure causes less melt and water to be swept out of the vessel by the escaping steam. For example, only 19% of the melt remains in the vessel after 1 second for a pressure of 0.1MPa, compared to virtually all the melt for pressures greater than 6MPa. The data in the table shows that in all cases approximately 70% of the water remains in the vessel after 1 second. As the pressure is increased a

greater mass of water is vaporised but less is swept out of the vessel because of the reduced steam flow.

Figure 4.3 shows the spatial variation of the volume fractions of steam and melt after one second. The figure shows that for low pressures ($\leq$ 1MPa) the melt is virtually uniformly distributed throughout the mixing vessel, but at higher pressures a pool of melt forms at the base of the vessel and less melt is swept upwards by steam. The steam volume fraction is greater than 40% over most of the vessel, except for a region 0.2m deep in the bottom of the water pool. In this region a mixture of all 3 phases exists for pressures of 6MPa and above. For lower pressures virtually no melt reaches the base of the vessel.

5. Discussion and Conclusions

A numerical scheme has been developed which can model transient one-dimensional mixing flows, including the effect of a phase change. At present somewhat arbitrary constitutive relationships for heat transfer and momentum exchange between phases have been employed. However, model predictions are in good agreement with results from a one-dimensional mixing experiment. This suggests that the constitutive relations may be predicting heat transfer rates and momentum relaxation times which are roughly of the magnitude needed to account for the experimental data available to date. It is a particular design feature of this code that one can work with virtually arbitrary constitutive relations subject only to certain very general restrictions. Thus, as more experimental or theoretical information becomes available on particle length scales, drag coefficients and heat transfer correlations, the calculations can be readily improved.

This is the first one-dimensional transient mixing model (to the authors' knowledge) which solves Eulerian conservation equations to describe the hydrodynamics of three components. Previous models have either relied on empirical correlations determined from experiments [12] or assumed homogeneous flow of the vapour and liquid coolant [10]. The studies presented in this paper show that the assumption of homogeneous flow is clearly unrealistic at low pressures and suggest that it could be

misleading to extrapolate experimental results obtained at one pressure to a different pressure.

It is intended to extend the present model to two-dimensions. This would allow comparison with experiments where the melt is poured into the coolant in the form of a jet which only occupies a small fraction of the vessel cross-section. In this situation, the steam can escape around the sides of the mixture and so is likely to cause less levitation of the melt and liquid.

In addition, improved constitutive relations are being developed.

Acknowledgements

The authors would like to thank Dr.F.Briscoe and Mr.I.Cook for valuable suggestions leading to the improvement of this paper.

References

[1] Thyagaraja, A, Fletcher, D.F. and Cook, I, One dimensional calculations of two-phase mixing flows. Culham Laboratory report CLM-P770 (1986).

[2] Hestroni, G (Ed) Handbook of multiphase flow systems, Hemisphere Publishing Corporation, Washington, (1982).

[3] Colgate, S.A, and Sigurgeirsson, T, Dynamic mixing of water and lava, Nature, 244, p.552-555 (1973).

[4] Gittus, J.H.(Ed.), Report on PWR Degraded Core analysis, UKAEA report NDR-610(s), Chapter 5, 1982.

[5] Fletcher, D.F., A Review of coarse mixing models. Culham Laboratory report CLM-R251(1985).

[6] Green, G.A, Ginsberg, T. and ,Tut, N.K, BNL severe accident sequence experiments and analysis program, in proceedings of the 12th NRC water reactor information meeting, Gaitisburg, 1984, Volume 3, 1985.

[7] Witte, L.C., Film boiling from a sphere, I & E C Fundamentals, 7, p.517-518 (1968).

[8] Chu, C.C.and Corradini, M.L., One-dimensional transient model for fuel-coolant fragmentation and mixing analysis. In proceedings of International ANS/ENS topical meeting on thermal reactor safety, San Diego, USA, 2-6 February, 1986.

[9] Bankoff, S.G. and Han, S.H., Mixing of molten core material and water. Nuc. Sci. and Eng., 85, p.387-395 (1983).

[10] Bankoff, S.G. and Han, S.H, An unsteady one-dimensional two-fluid model for fuel-coolant mixing in an LWR meltdown accident. Presented at the US-Japan Seminar on Two-phase Flow Dynamics, Lake Placid, NY, July 29-August 3, 1984.

[11] Bird, M.J, An experimental study of Scaling in core melt/water interactions. Paper presented at the 22nd National Heat transfer Conference, Niagara Falls, 5-8 August,1984.

[12] Corradini, M L and Moses, G.A, A Dynamic model for fuel-coolant mixing. Presented at the International Meeting on Light Water Reactor Severe Accident Evaluation, Cambridge, Massachusetts, 1983.

[13] Fletcher, D.F. Assessment and development of the Bankoff and Han coarse mixing model. Culham Laboratory report CLM-R252 (1985).

[14] Harlow, F H and Amsden, A A, Flow of interpenetrating material phases. J Comp Phys, 18, p.440-465 (1975).

APPENDIX 1: Constitutive Relations

In this Appendix we discuss the forms chosen as an interim measure for the interfacial drag laws and the vaporisation rate.

The drag law used was that proposed by Harlow and Amsden [14] from which, neglecting the viscous terms, we have

$$F_{ij} = 3/4\ \alpha_i \alpha_j \rho_i \rho_j \frac{C_{Dij} D_i D_j}{(\rho_i D_j + \rho_j D_i)} \left(\frac{1}{D_i} + \frac{1}{D_j}\right)^2 |U_i - U_j| (U_i - U_j) \qquad (A1.1)$$

where:-

C_{Dij} is the drag coefficient between phases i and j

D_i, D_j are the length-scales of phases i and j

Harlow and Amsden give no justification for the form of the above equation, other than that it reduces to the correct form as one phase becomes very dilute i.e. as $\alpha_i \to 1$ and $D_i \to \infty$

$$F_{ij} \to 3/4\ \alpha_j \rho_i C_{Dij} |U_i - U_j| (U_i - U_j) / D_j \qquad (A1.2)$$

In future work any changes to F_{ij} will always be expressible in the form

$$F_{ij} = \alpha_i \alpha_j \rho_i \rho_j h(\alpha_i, \alpha_j, \rho_i, \rho_j, D_i, D_j) |U_i - U_j| (U_i - U_j) \qquad (A1.3)$$

The mass production rate of vapour was expressed in the general form

$$\dot{m}_S = \alpha_W \alpha_M \rho_S \lambda \qquad (A1.4)$$

and thus it is required to establish an expression for λ. Assuming the melt particles to be in the form of spheres with a diameter D_M, then there are $\alpha_M / 1/6 \pi D_M^3$ spheres per unit volume and if q is the heat flux per unit

area (typically q is the sum of a radiation heat flux and a film boiling heat flux [13]), which is determined by the physics of the situation of interest, the total heat transfer rate Q per unit volume is given by

$$Q = 6q\ \alpha_M/D_M \qquad \text{(A1.5)}$$

Assuming that the liquid is saturated and the heat transfer produces saturated steam, then the mass of steam produced is Q/h_{fg}, where h_{fg} is the latent heat of vaporization. Multiplying this by α_W to account for the reduction in heat transfer as more steam is produced, shows that λ should take the following form

$$\lambda = 6q/D_M h_{fg} \rho_S$$

The assumption that the heat flux should be weighted by a factor α_W is somewhat arbitrary (it might for example be a nonlinear function of α_W) but is allows qualitatively for the reduction in heat transfer which must occur as the water volume fraction falls. Again it is intended to examine the validity of this assumption in future work.

PRESSURE (MPa)	0.1	1.0	6.0	15
Total mass of steam produced after one second (kg)	98	248	527	891
Total volume of steam produced after one second (m^3)	163	47	17	9.2
Typical steam exit velocity (m/s)	50	18	7	3
Typical water exit velocity (m/s)	4	3	2	1
Fraction of melt remaining after one second	19%	51%	97%	100%
Fraction of water remaining after one second	79%	80%	76%	65%
Time for melt front to reach the vessel base (s)	> 1	0.85	0.75	0.7

Table 4.1: The Effect of Pressure

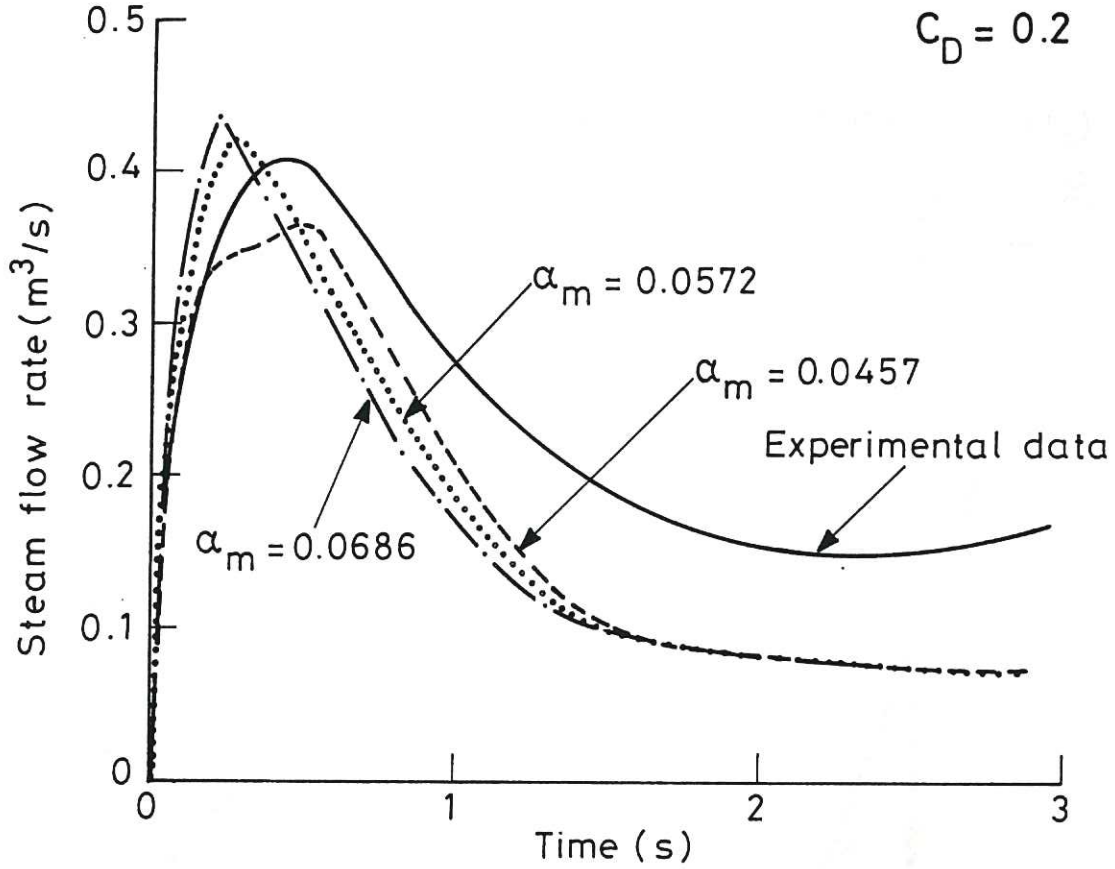

(a) The effect of Initial Melt Fraction

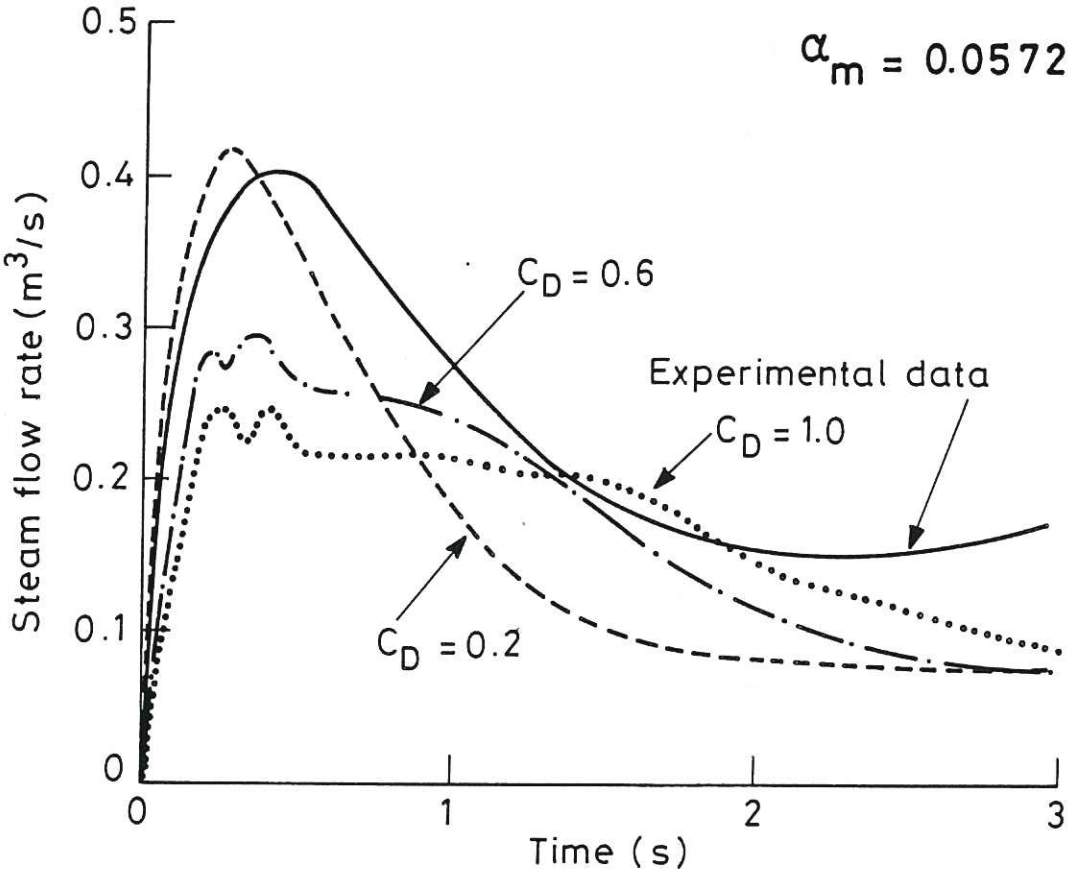

(b) The effect of C_D

Figure 4.1. Comparison of steam flow rates with calculations for the BNL experiments.

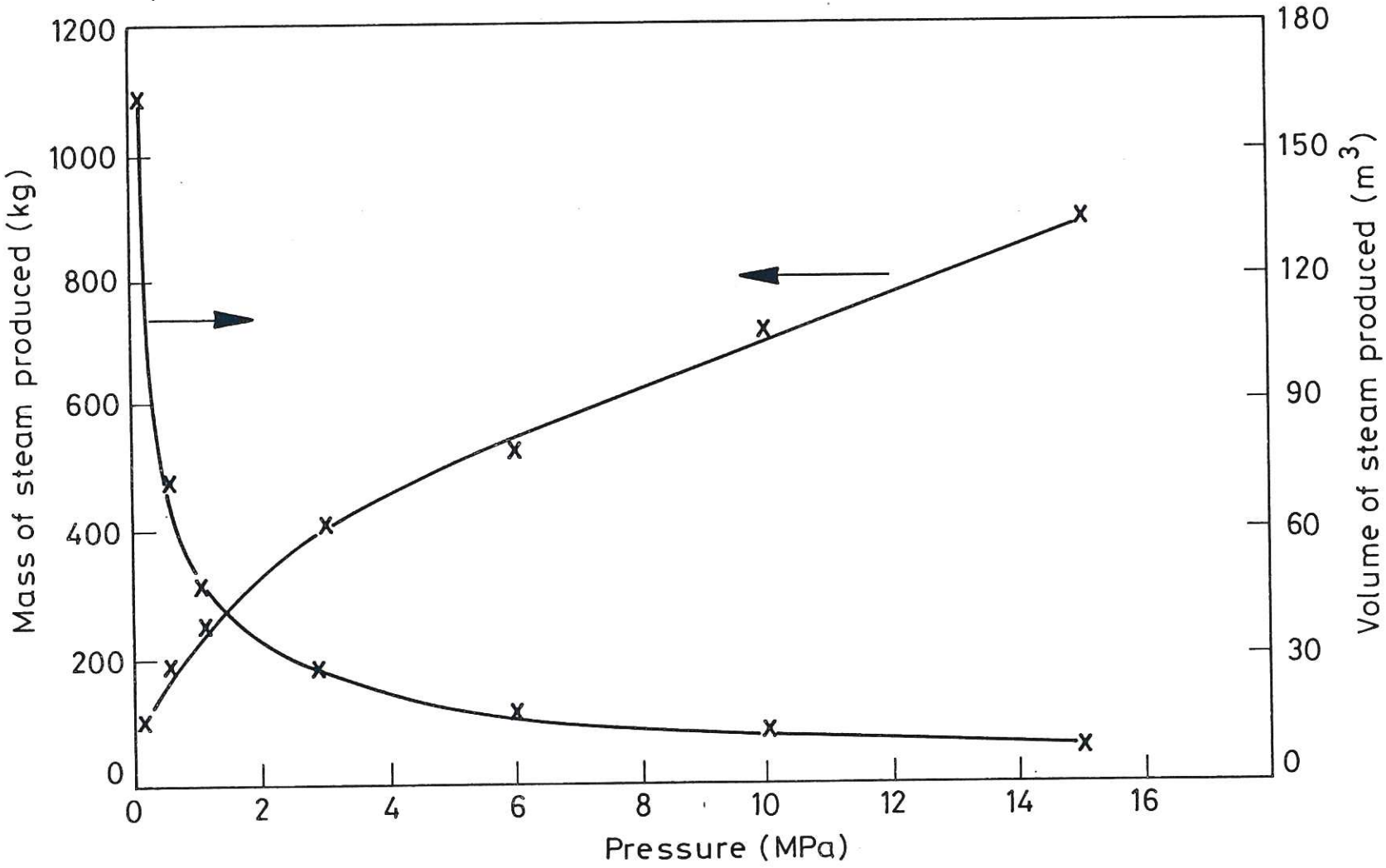

Figure 4.2. The effect of pressure on vapour production

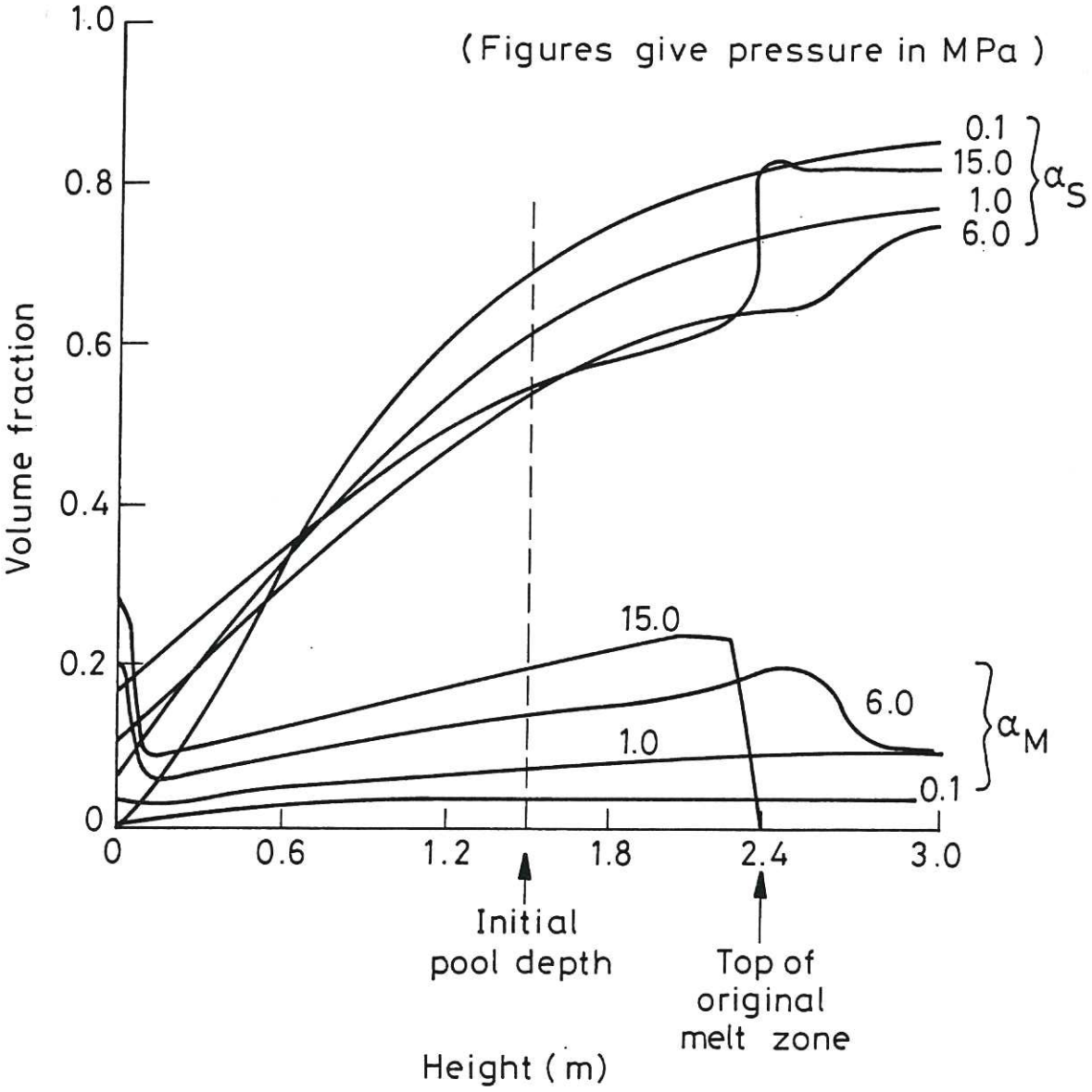

Figure 4.3. The volume fraction distributions one second after the start of mixing.